PHOTOSYNTHETICA
International Journal for Photosynthesis Research

DOI 10.32615/ps.2025.006 PHOTOSYNTHETICA 63 (1): 51-63, 2025

Special issue in honor of Prof. Hartmut Karl Lichtenthaler

Response of leaf internal CO_2 concentration and intrinsic water-use efficiency in Norway spruce to century-long gradual CO_2 elevation

J. ŠANTRŮČEK[*,+], J. KUBÁSEK[*], J. JANOVÁ[*], H. ŠANTRŮČKOVÁ[*], J. ALTMAN[**,***], J. TUMAJER[#,##], M. HRÁDKOVÁ[*,**], and E. CIENCIALA[#]

Faculty of Science, University of South Bohemia, Branišovská 31, 370 05 České Budějovice, Czech Republic[*]
Institute of Botany, AS CR, Zámek 1, 252 43 Průhonice, Czech Republic[**]
Faculty of Forestry and Wood Sciences, Czech University of Life Sciences Prague, Kamýcká 129, 165 21 Prague 6 – Suchdol, Czech Republic[***]
IFER – Institute of Forest Ecosystem Research, Čs. armády 655, 254 01 Jílové u Prahy, Czech Republic[#]
Department of Physical Geography and Geoecology, Faculty of Science, Charles University, Albertov 6, 12843 Prague, Czech Republic[##]

Abstract

The strategies of Norway spruce [*Picea abies* (L.) Karst.] to increasing atmospheric CO_2 concentration (C_a) are not entirely clear. Here, we reconstructed centennial trajectories of leaf internal CO_2 concentration (C_i) and intrinsic water-use efficiency (WUE_i) from the amount of ^{13}C in tree-ring cellulose. We collected 57 cores across elevations, soil, and atmospheric conditions in central Europe. Generally, WUE_i and C_i increased over the last 100 years and the C_i/C_a ratio remained almost constant. However, two groups were distinguished. The first group showed a quasi-linear response to C_a and the sensitivity of C_i to C_a ($s = dC_i/dC_a$) ranged from 0 to 1. Trees in the second group showed nonmonotonic responses with extremes during the peak of industrial air pollution in the 1980s and s increase from –1 to +1.6. Our study shows a marked attenuation of the rise in WUE_i during the 20th century leading to invariant WUE_i in recent decades.

Keywords: carbon dioxide enrichment; photosynthesis; *Picea abies*; stable carbon isotopes; tree rings; water-use efficiency.

Highlights

- The centennial rise in $[CO_2]$ increased intrinsic water-use efficiency (WUE_i) by 46%
- The ratio between leaf internal and external $[CO_2]$ was almost constant in some trees
- The sensitivity of WUE_i to atmospheric $[CO_2]$ decreased over the last century

Received 1 October 2024
Accepted 10 February 2025
Published online 13 March 2025

[+]Corresponding author
e-mail: jsan@umbr.cas.cz

Abbreviations: a – $^{13}CO_2$ *vs.* $^{12}CO_2$ fractionation during diffusion; b – $^{13}CO_2$ *vs.* $^{12}CO_2$ fractionation during carboxylation by Rubisco; C_a – CO_2 concentration in atmosphere; C_i – intercellular CO_2 concentration; E – transpiration rate; EA – elemental analyser; g_s – stomatal conductance; g_{sc} – stomatal conductance for CO_2; g_{sw} – stomatal conductance for water; IRMS – isotope ratio mass spectrometer; J_{max} – the maximum rate of electron transport; l – the slope of the WUE_i *vs.* C_a relationship ($dWUE_i/dC_a$); P_N – net photosynthetic rate; R – carbon isotope ratio ($^{13}C/^{12}C$); s – slope of the C_i *vs.* C_a relationship (dC_i/dC_a); $V_{c\,max}$ – the maximum rate of carboxylation; VPD – vapour pressure deficit; WUE – water-use efficiency (P_N/E); WUE_i – intrinsic water-use efficiency (P_N/g_{sc}); $\delta^{13}C$ – the relative difference in R between sample (air, wood, *etc.*) and standard; $\Delta^{13}C$ – discrimination of $^{13}CO_2$ against $^{12}CO_2$ in a given process (*e.g.*, during CO_2 assimilation).

Acknowledgements: Czech Science Foundation (14-12262S, 18-14704S), Ministry of Education Youth and Sports of the Czech Republic (Czech Research Infrastructure for Systems Biology, C4SYS, LM2015055 to JS, JK, JN), and long-term research development project no. RVO 67985939 of the Czech Academy of Sciences are acknowledged for their support.
We thank Ladislav Marek and Jiří Květoň for performing the carbon isotope analyses, and Petra Fialová and Marcela Cuhrová for technical assistance. We also thank our colleagues from IFER who assisted during fieldwork and Gerhard Kerstiens (Lancaster) for language revisions and valuable comments.
Conflict of interest: The authors declare that they have no conflict of interest.

Introduction

Carbon assimilation, growth, and reproduction of terrestrial plants are often limited by the availability of water. Land plants have evolved stomata to cope with the lack of soil water in a way that maximizes carbon gained over some time in fluctuating environments (Cowan and Farquhar 1977, Vico *et al*. 2013). To realize this strategy, stomata respond to a range of environmental signals by opening (*e.g.*, in response to increased light or air humidity or decreased leaf internal CO_2 concentration) or closing (*e.g*., at dusk or in response to water shortage or a rise in CO_2 concentration) over a short period. Over long-term leaf development, the number of stomata per unit leaf area (stomatal density) and the size of stomata also vary in response to the light and CO_2 environment (Lake *et al.* 2001, Lake and Woodward 2008). Thus, the environment modulates carbon assimilation at the leaf-to-canopy level through the number and opening of stomata, and stomata are in turn involved in controlling global carbon and water cycles (Hetherington and Woodward 2003, Jasechko *et al.* 2013). For example, partial closure of stomata due to increasing CO_2 concentration in the Earth's atmosphere leads to reduced transpiration rates in temperate and boreal forests in the Northern Hemisphere (Keenan *et al.* 2013), which leaves more water in the soil and can increase continental water runoff (Betts *et al.* 2007). In turn, elevated CO_2 can alleviate the substrate deficiency for carboxylation in the chloroplasts and the "CO_2 fertilisation" effect helps plants to improve the trade-off between water loss and CO_2 uptake (Ainsworth and Rogers 2007).

Water and CO_2 diffuse between the leaf and the atmosphere in opposite directions, with water vapour being 1.6 times faster than CO_2 due to its lower molecular mass. In addition, the diffusive flux of water through stomata (*i.e*., transpiration) is, by differences in CO_2 and water concentration gradients, 2–3 orders of magnitude greater than that of CO_2 assimilated in photosynthesis. Due to these physical constraints, the water-use efficiency (WUE), the ratio of assimilated CO_2 (P_N) to water vapour loss (E), is low. Typically, WUE in temperate forests ranges from 1.5 to 20 mmol(CO_2) mol^{-1}(H_2O) (Ponton *et al.* 2006, Yu *et al.* 2008, Hoshika *et al.* 2012, Brümmer *et al.* 2012), depending on the water vapour pressure deficit in the ambient air (VPD), leaf temperature, light, and other environmental factors that drive E and P_N. Gas-exchange measurements allow the calculation of stomatal conductance for the diffusion of water vapour (g_{sw}), a measure that reflects stomatal aperture, size, and density on the leaf surface, the main physiological parameters controlling E. Substitution of E with g_s in the WUE lets us factor-out VPD and obtain a "more physiological" characteristic of plant water use, the so-called intrinsic water-use efficiency, $WUE_i = P_N/g_s$. WUE_i has two positive properties: first, it can be assessed without knowledge of VPD, and second, it is a simple function of the leaf's internal CO_2 concentration (C_i), which is imprinted in the relative abundance of ^{13}C isotope in assimilates (*see* next paragraph and "Materials and methods" for more details). Both properties make WUE_i a favourite parameter for studying the acclimation of plants (especially trees) and ecosystems to climate change (Miller-Rushing *et al.* 2009, Gagen *et al.* 2011, Peñuelas *et al.* 2011), drought response strategies (Cavender-Bares and Bazzaz 2000), and impacts of air or soil pollution (Šantrůčková *et al.* 2007, Guerrieri *et al.* 2011). (Note that the term acclimation is used here for environmentally inducible physiological responses that are limited to the lifetime of an individual tree.)

Trees in seasonal climates "archive" physiological responses to variation in environmental conditions in their tree rings, allowing us to study precisely defined periods spanning from decades to many centuries (Fritts 1976, Schweingruber 1996). Cellulose and other wood components are deposited in the trunks year by year at a rate that varies with the season in a specific manner, forming tree rings of discernible width, density and chemical composition. The chronology of the carbon isotopic composition ($\delta^{13}C$) of the wood of successive tree rings provides a tool to relate processes within the tree to changing environmental conditions. The tool is not biased by the age of the trees after the juvenile phase [Loader *et al.* (2007) but *see* also Brienen *et al.* (2017)]. Discrimination against $^{13}CO_2$ during CO_2 transport to and during carboxylation in the chloroplasts is the primary cause of ^{13}C depletion in sugars, cellulose, and finally in wood (Farquhar *et al.* 1989, Gessler *et al.* 2014). The isotopic shift between atmosphere and wood ($\Delta^{13}C \cong \delta^{13}C_{air} - \delta^{13}C_{wood}$) is, with approximations, proportional to the CO_2 concentration in the leaf interior (C_i), weighted by the rate of net photosynthesis (P_N) and integrated over the time of photosynthetic CO_2 fixation and the tree ring formation, and inversely proportional to the atmospheric CO_2 concentration (C_a) (Farquhar and Sharkey 1982). Therefore, isotopic discrimination $\Delta^{13}C$ can serve as a proxy for estimating C_i, assuming C_a is known. The value of C_i is a "set point" that balances CO_2 influx through variable stomatal conductance with CO_2 consumption in light-dependent photosynthetic carboxylation. C_i chronologies derived from $\Delta^{13}C$ reconstructed for trees grown under rising atmospheric CO_2 concentration in recent decades and centuries typically show a smaller increase in C_i than in C_a, indicating enhanced water-use efficiency (Saurer *et al.* 2014, Köhler *et al.* 2016).

It is well known that plants acclimate to elevated atmospheric CO_2 by reducing stomatal conductance and often by reducing stomatal density on new leaves (Ainsworth and Rogers 2007). As a result, C_i decreases due to the lower g_s, which can be counterbalanced by elevated ambient CO_2 concentration. Four different types of C_i responses to rising C_a concentrations have been reported: (*1*) C_i remains nearly constant despite increasing C_a (Francey and Farquhar 1982, Waterhouse *et al.* 2004, Keenan *et al.* 2013) or (*2*) C_i follows the increase in C_a. In the latter case, the plant either (*2*-a) "actively" controls C_i so that the C_i/C_a ratio remains constant (Sage 1994, Saurer *et al.* 2004, Andreu-Hayles *et al.* 2011, Frank *et al.* 2015, Köhler *et al.* 2016, Keller *et al.* 2017), or

(*2*-b) the increments in C_i and C_a are equal, *i.e.*, C_i follows C_a "passively" and the difference between C_a and C_i does not change (Andreu-Hayles *et al.* 2011), or (*2*-c) C_i can even temporarily increase faster than C_a for a transient period, so that C_i/C_a increases and $C_a - C_i$ diminishes (Boettger *et al.* 2014, Čada *et al.* 2016).

What can we learn from the C_i *vs*. C_a relationship about plant carbon assimilation relative to water consumption? Can the apparent homeostasis of C_i, the C_i/C_a ratio or the $C_a - C_i$ difference be affected by a centennial increase in C_a? To answer these questions, we analysed the abundance of ^{13}C in the cellulose of tree rings and reconstructed 33- to 100-year-long chronologies of C_i in spruce trees. We have used a large set of Czech forest inventory data on vegetation and soil properties acquired from sampling plots distributed across the country. We expected C_i to rise along with C_a for a century. Furthermore, the $C_a - C_i$ difference was expected to increase, indicating a continuous increase in the availability of CO_2 for carboxylation and/or a decrease in water loss. We also hypothesised that the sensitivity of WUE_i to a life-long gradual elevation of atmospheric CO_2 concentration will decrease depending on the WUE_i history of individual trees.

Materials and methods

Sampling sites: The sampling sites were distributed over the whole territory of the Czech Republic (CR), where Norway spruce, *Picea abies* (L.) Karst., is grown extensively from low (~250 m a.s.l.) to high (~1,300 m a.s.l.) altitudes. The application of a regular grid of 7 × 7 km^2 squares produced 1,599 locations covering the entire Czech territory (79,886 km^2). The sampling was organised as part of the *CzechTerra landscape* inventory project (Cienciala *et al*. 2016). A circular sampling area with a radius of 12.6 m (500 m^2) was defined at each site with forest or other forested areas (n = 604). Spruce cores were always taken next to the plot boundary (from the outside). For isotopic analysis, a set of 66 thoroughly cross-dated cores of trees from 60 forest plots was selected to cover the whole territory and the different elevations (Fig. 1). In general, one tree sample per plot was selected and analysed except for three plots where three individual trees were analysed. The 60 selected sampling sites were distributed over the entire CR area and ranged in altitude from 232–1,060 m a.s.l. (Fig. 1). Of the 60 sampling sites, 8, 32, and 20 plots were located below 400 m a.s.l., between 400 and 700 m a.s.l., and above 700 m a.s.l., respectively.

Annual temperature means at the different sampling sites over the period 1961–2014, for which meteorological data were available, ranged from 3.9°C to 8.7°C (10.9–16.2°C for May to September, M–S), and precipitation was between 507 mm and 1,308 mm (292–654 mm in M–S). Air temperature, precipitation and SPEI [SPEI-12; multi-scalar drought index based on precipitation and temperature data (Vicente-Serrano *et al.* 2010)] during the last hundred years are shown separately for winter, spring, summer and the whole year in Fig. 1S (*supplement*). The range of site-specific mean annual deposition rates of SO_4^{2-}, NO_3^-, and NH_4^+ over the same period was 40.2–98.5 mmol m^{-2} yr^{-1}, 5.9–15.9 kg N ha^{-1} yr^{-1}, and 11.1–21.4 kg N ha^{-1} yr^{-1}, respectively (*see* Fig. 2S, *supplement* for detailed deposition data). The data on environmental parameters were taken from Šantrůčková *et al.* (2019).

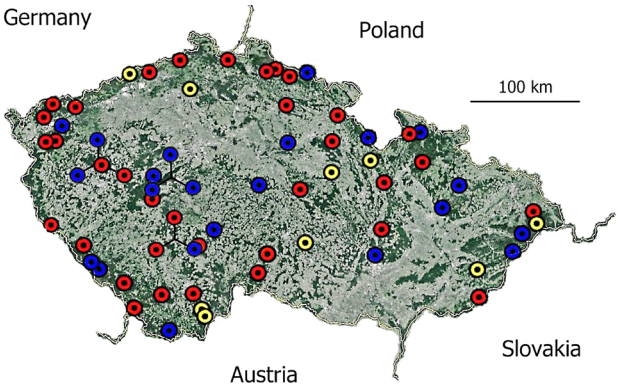

Fig. 1. Location of sampling sites in forests and woodlands of the Czech Republic. *Blue* and *red symbols* indicate the positions of the 57 sampled and analysed cores (note that at three locations with points connected by an inverted Y, three trees per site were analysed so there were 51 sites with sampled and analysed cores) and the type of $\Delta^{13}C$ time course: *blue* for Response Type 1 (RT1), *red* for Response Type 2 (RT2). The nine *yellow circles* indicate the position of tree-ring series shorter than 33 years that were analysed but not included in the data set evaluated here. *Dark grey areas* indicate larger forest complexes on an orthophoto image of the Czech Republic.

Sampling, cross-dating: From each plot, three to eight wood cores of *P. abies* were taken (one core per tree). Coring was carried out at breast height (1.3 m) using a steel borer. All cores were dried and a thin layer of wood was sliced off each core with a core microtome (Gärtner and Nievergelt 2010) to make the tree-ring boundaries easier to detect. The rings were counted from the pith to the bark and tree-ring widths were measured to the nearest 0.01 mm using the *TimeTable* measuring device and the *PAST4* software (http://www.sciem.com/). The ring sequences were visually cross-dated using the individual patterns of the wide and narrow rings (Yamaguchi 1991). Cross-dating was verified by the percentage of parallel variation [Gleichläufigkeit; *see* Eckstein and Bauch (1969)] and the similarity of growth patterns between individual series [*Baillie–Pilcher*'s *t*-value; *see* Baillie and Pilcher (1973)]. A total of 1,202 time series were successfully cross-dated [for details *see* Altman *et al.* (2017), Tumajer *et al.* (2017)]. For this study, only the trees that showed the highest cross-correlation with the mean site chronology were selected. To avoid the bias in isotope discrimination occurring during the juvenile period, the first 30 years in each core selected for isotopic analysis were ignored. In addition, only cores with more than 33 additional tree rings were analysed. In total, 57 wood cores from 51 different plots were analysed in this study (*see* the red and blue sites in Fig. 1).

Extraction of α-cellulose: The latewood in the tree rings was separated year by year with a scalpel. Each single

cut was enclosed in a Teflon pocket (*F57* 25 µm porosity, *ANKOM*, USA). For 11 of the wood cores investigated, we pooled the samples for 5-year periods, while the others were analysed at a one-year resolution. Because of the small amount of material, we extracted α-cellulose from the entire nonhomogenized wood sample, using a modified version of the method of Loader *et al.* (1997). Briefly, samples were exposed to a 5% NaOH solution for 4 h (at 60°C, renewing the solution after 2 h), which removed tannins, lipids, resins, and hemicelluloses. Then the samples were washed with hot deionized water (3 times) and bleached in an acetic acid solution containing 7% $NaClO_2$ (pH 4–5) at 60°C for 25 d. The bleaching solution was changed every 7–10 d. After the lignin was removed by bleaching, the samples were washed 3 times with hot distilled water and dried at 50°C for 12 h. After drying, the cellulose samples were transferred from their Teflon pockets to vials filled with 1 ml of distilled water, stored overnight in a refrigerator and homogenized with an ultrasonic homogenizer (*Bandelin Sonopuls HD2200*, Germany) according to Laumer *et al.* (2009). The homogenized cellulose fibers were dried at 80°C for 48 h.

Carbon isotopes, determination of leaf physiological parameters: The relative abundance of ^{13}C over ^{12}C ($\delta^{13}C$) in extracted α-cellulose was measured using isotope ratio mass spectrometry (IRMS). The dried samples were packed in tin capsules and oxidised in a stream of pure oxygen by flash combustion at 950°C in the reactor of an elemental analyser (EA) (*NC 2100 Soil*, *ThermoQuest CE Instrument*s, Rodano, Italy). After CO_2 separation, the $^{13}C/^{12}C$ ratio (R) was detected *via* continuous flow IRMS (*Delta plus XL*, *ThermoFinnigan*, Bremen, Germany) connected online to the EA. The $\delta^{13}C$, expressed in ‰, was calculated as the relative difference of sample and standard R: $\delta^{13}C = (R_{sample}/R_{standard} - 1) \times 1{,}000$ with VPDB (*IAEA*, Vienna, Austria) as the standard. The standard deviations of the analyses were between 0.05 and 0.1‰.

The carbon isotope composition of the sugars synthesized during photosynthesis is imprinted with a certain offset (*see* below) in the cellulose and the wood produced. From the $\delta^{13}C$ value of α-cellulose, we reconstructed three parameters related to leaf physiology: (*1*) the discrimination of ^{13}C against ^{12}C ($\Delta^{13}C$), (*2*) the leaf internal CO_2 concentration (C_i) weighted by the photosynthetic rate and integrated over periods of active photosynthesis during the late season in a given year, and (*3*) the intrinsic water-use efficiency (WUE_i). The carbon isotopic composition of foliage was reconstructed using the relationship $\delta^{13}C_{foliage} = 1.0523 \times \delta^{13}C_{cellulose} - 0.205$ according to Gebauer and Schulze (1991) and expressed as discrimination against ^{13}C in the atmosphere ($\Delta^{13}C$) as follows:

$$\Delta^{13}C\left[‰\right] = \frac{(\delta^{13}C_{air} - \delta^{13}C_{foliage})}{1 + \frac{\delta^{13}C_{foliage}}{1000}} \qquad \text{(Eq. 1)}$$

where $\delta^{13}C_{air}$ and $\delta^{13}C_{foliage}$ are the relative isotopic compositions of the atmosphere and foliage, respectively. $\delta^{13}C_{air}$ has been anthropogenically altered during the last century by increasing the fraction of $^{12}CO_2$ in the atmosphere. Therefore, we have corrected $\delta^{13}C_{air}$ for this phenomenon (McCarroll and Loader 2004). The seasonally integrated leaf internal CO_2 concentration (C_i) was estimated using the following simplified linear relationship (Farquhar *et al.* 1982):

$$C_i = C_a \frac{\Delta^{13}C - a}{b - a} \qquad \text{(Eq. 2)}$$

where C_a is the atmospheric CO_2 concentration in the year in question, a and b are the fractionation factors for the diffusion of CO_2 through stomata (4.4‰) and during photosynthetic carboxylation by Rubisco and PEP-carboxylase (27‰), respectively. C_a values were obtained from published measurements of CO_2 in the atmosphere (Keeling and Whorf 2004) and in gas bubbles in ice cores (Francey *et al.* 1999). The intrinsic water-use efficiency [WUE_i, µmol(CO_2) $mol^{-1}(H_2O)$], the ratio of carbon assimilation rate (P_N) to stomatal conductance for water vapour (g_{sw}), was calculated using the C_i values obtained from $\Delta^{13}C$ and Eq. 2 as follows:

$$WUE_i = \frac{P_N}{g_{sw}} = \frac{(C_a - C_i)}{1.6} = C_a\left(1 - \frac{C_i}{C_a}\right)\frac{1}{1.6} \qquad \text{(Eq. 3)}$$

where 1.6 is the ratio of the stomatal conductances for water and CO_2 (g_{sw}/g_{sc}), which is equal to the ratio of diffusivities of water and CO_2 in air (D_w/D_c).

Conceptual model of the responses of C_i and WUE_i to increasing atmospheric CO_2 concentrations: The relationship between WUE_i, defined as 1/1.6 of the difference in CO_2 concentration across stomata ($C_a - C_i$) in Eq. 3, and atmospheric CO_2 concentration can be used as an indicator of the particular strategy that plants adopt in the world of elevated CO_2. The strategy, *i.e.*, the strength of C_i control, reflects the availability of resources (water, nitrogen, CO_2) and the coordination of stomata and photosynthetic machinery in their utilisation (*see* below for more details). Four types of strategies have been identified (*e.g.*, Saurer *et al.* 2004, Arco Molina *et al.* 2024). Plants can respond to increasing C_a by: (*A*) keeping C_i approximately constant, (*B*) adjusting C_i to a certain value so that the C_i/C_a ratio remains unchanged, (*C*) increasing C_i at the same rate as C_a and thus keeping the difference ($C_a - C_i$) constant, or (*D*) temporarily increasing C_i by increments which are higher than that of C_a. The four types of behaviour are illustrated in Fig. 2 as plots of WUE_i *vs.* C_a, with the slopes decreasing from *A* to *D*. In turn, the slopes s of the increase in C_i with rising C_a become steeper from *A* to *D* (*see* insets in Fig. 2). The strength with which plants control C_i, the gain of the closed loop involving stomata and photosynthesis (Farquhar *et al.* 1978), can be visualized by the slope s of the C_i *vs.* C_a relation ($s = dC_i/dC_a$). Usually, s is in the range between 0 and 1. The capacity to control C_i (C_i homeostasis) is inversely proportional to s: plants with $s = 0$ "protect" the leaf so strongly that no changes in C_i arise in response to fluctuating C_a; thus, they exhibit

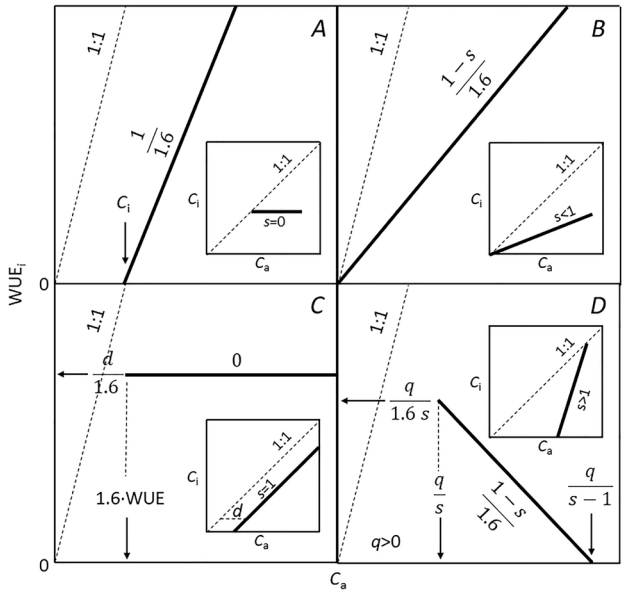

Fig. 2. Typical responses of intrinsic water-use efficiency (WUE_i) and leaf internal CO_2 concentration (C_i) to changes in atmospheric CO_2 concentration (C_a). Four simple scenarios (*A–D*) of the responses of C_i (*bold lines* with slope *s* in the insets) and WUE_i (*bold lines* with slope *l* in the main plots) to increasing C_a are presented. CO_2 consumption by photosynthesis and CO_2 supply through the stomata can (*A*) keep C_i constant, (*B*) keep the C_i/C_a ratio constant at a value less than one (C_i increases slower than C_a), (*C*) keep the difference $d = C_a - C_i$ constant (C_i increases at the same rate as C_a), or (*D*) reduce the difference $C_a - C_i$ at a rate proportional to *s* and with an offset *q* (C_i increases faster than C_a). All models of C_i behaviour assume that $C_i \leq C_a$; *q* is defined as $-C_i$ at $C_a = 0$. WUE_i was calculated as $(C_a - C_i)/1.6$ (*see* Eq. 3 in "Materials and methods"). WUE_i increases with C_a (*A*,*B*), remains constant (*C*) or decreases with C_a (*D*). The sensitivity *l* of WUE_i to C_a declines from (*A*) to (*D*).

more of C_i homeostasis than plants with $s = 1$, in which C_i "passively" follows C_a (and $C_a - C_i$ remains constant). Therefore, *s* may indicate acclimation to C_a elevation through changes in the sensitivity of stomata and photosynthesis.

Data processing and statistics: The primary $\delta^{13}C$ data were tested for outliers and missing values (*Grubbs*' test). Those which did not pass the test (<1% of the total) were interpolated using neighbouring values and replaced. The 57 series longer than 33 years were used for the ^{13}C analyses of the latewood. Of these chronologies, 47 were analysed with a 1-year resolution and 10 as 5-year pooled samples. The pooled series were included in estimating long-term trends (MA10) but excluded from the analyses of interannual high-frequency signals. The C_i series were individually plotted against C_a and fitted with polynomial functions. The values of the slope *s* (dC_i/dC_a) for each individual year and series were calculated as derivatives of the polynomials. The WUE_i series was smoothed by calculating 10-year moving averages (MA10). For significance tests with nonnormal data distributions, the nonparametric rank-based *Spearman* correlation was used. The software package *Statistica 13* (*Dell Inc*., Tulsa, USA) and *SigmaPlot 13.0* were used.

Visual inspection of the $\Delta^{13}C$ time series identified two distinct groups of trees with contrasting long-term trends. Principal component analysis (PCA) was used for the quantitative identification of clusters with similar trends (Buras *et al.* 2016). The first principal component captures the common part of the variability, while the second principal component captures the tree-specific variability. This resulted in two clusters (Response Types, RTs) with positive and negative values for the second principal component, respectively. However, since both extremely short and long series are present in our dataset, we performed PCA only for the period since 1981 (*i.e.*, for the common time span of all trees). The assignment of long series (6 out of 57 series) to individual clusters in earlier periods was verified manually.

Results

$\Delta^{13}C$ time series: The $\Delta^{13}C$ values varied between 12.3 and 21.1‰ (16.5 ± 1.5‰, mean ± SD) in the whole dataset (n = 3,261) and met the criteria for a normal distribution (K-S test). Fig. 3*A* shows means and quantiles for each year and all series represented in the respective year (the uncorrected $\delta^{13}C$ values of the cellulose samples are shown in Fig. 3S, *supplement*). Two virtually distinct long-term patterns of $\Delta^{13}C$ were readily visible in the primary data plots. The typical tree of the first group exhibited minimal long-term fluctuations in the moving averages (MA10) of $\Delta^{13}C$ compared to the interannual high-frequency signal. This group is referred to below as Response Type 1 (RT1). A typical series from the other group exhibited $\Delta^{13}C$ decline comparable to or higher than the high-frequency changes in 1920–1995. We denote this behaviour as Response Type 2 (RT2). RT1, consisting of 23 series (from 19 sites), showed only mild irregularities in MA10 values of $\Delta^{13}C$ over the last hundred years (Fig. 3*B*). In contrast, in RT2, consisting of 34 trees (from 32 sites), $\Delta^{13}C$ typically decreased by 2–3‰ after 1920 and tended to increase again between 1995–2014 (Fig. 3*C*). RT1 and RT2 trees did not show a distinctly different spatial distribution across the entire sampling area (*see* blue and red circles in Fig. 1) but RT1 trees were distributed in their $\Delta^{13}C$ and WUE_i according to the elevation gradient (*see* below).

Correlations between $\Delta^{13}C$ series: The inter-annual variability of $\Delta^{13}C$ may be environmentally driven, largely site-specific, and/or due to individual genetic differences. We tested site-specificity by correlating the complete $\Delta^{13}C$ series of three individual trees growing in the same sample plot. The correlation coefficients for the three cored trees (triplicates) from each of the three selected plots (plots nos. 165, 436, and 444) ranged from 0.68 to 0.84 (Fig. 4). By contrast, the correlation coefficients between series from randomly selected sites (each site correlated with all others, n = 990) ranged from –0.61 to +0.88 (the 5% and 25% quantiles, median, and 75% and 95% quantiles of the correlation coefficients were: –0.30, 0.02,

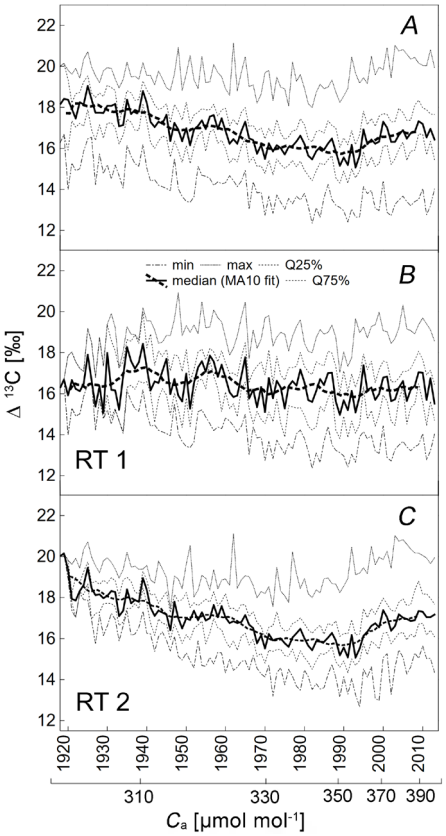

Fig. 3. Time course of the leaf-level $\Delta^{13}C$ in Norway spruce reconstructed from tree-ring $\delta^{13}C$ of late-wood cellulose. The medians and the 10-year moving averages of the median (*solid* and *dashed bold lines*, respectively) are shown together with the minima, maxima, 25% and 75% percentiles (*finer lines*; for the patterns, see inset in panel *B*) calculated for each year and all tree-ring series (cores). (*A*) Result for all 57 series investigated; (*B*) 23 series showing nearly invariant long-term courses of $\Delta^{13}C$ (Response Type 1, RT1); (*C*) the remaining 34 series showing substantial low-frequency $\Delta^{13}C$ depression with minimum values between 1965 and 1995 (Response Type 2, RT2). The results for the years before ca. 1940 should be treated with caution due to the scarcity of data.

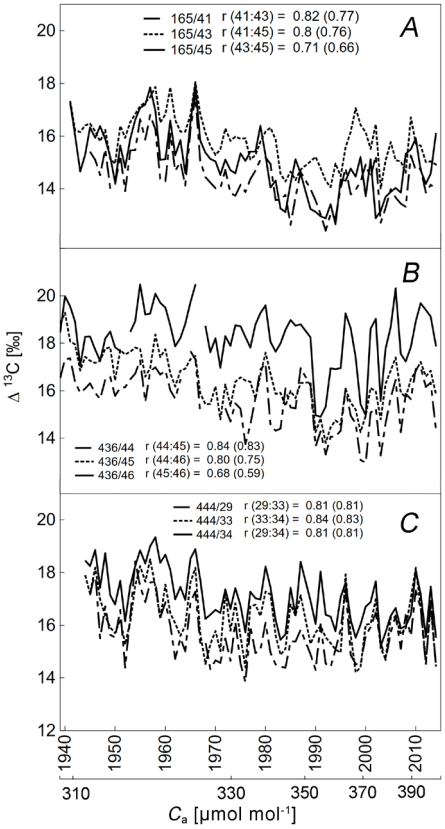

Fig. 4. Time courses of the leaf-level $\Delta^{13}C$ of trees growing at common sampling sites (triplications). Panels (*A*), (*B*), and (*C*) show data for three sites (plots nos. 165, 436, 444). $\Delta^{13}C$ series of three individual trees sampled on each plot are shown (trees nos. 41, 43, 45; 44, 45, 46; 29, 33, 34). The legends indicate the *Pearson* and *Spearman* correlation coefficients (in brackets) for all three pairs of series at each site. The parametric (*Pearson*) and rank-based (*Spearman*) correlation coefficients do not differ substantially, indicating a near-normal data distribution.

0.27, 0.45, 0.66, respectively). The correlation coefficients between the series obtained from trees grown on the same plot were all above 0.68 and thus within the top 5% of correlations between all pairs of series, indicating that environmental factors dominate over genetic differences in determining interannual variability.

Leaf intercellular CO_2 concentration, its ratio to atmospheric CO_2 (C_i/C_a) and the slope s (dC_i/dC_a): C_i values in RT1 increased quasilinearly with the increase in C_a from about 170 µmol mol^{-1} at the beginning of the last century to 210 µmol mol^{-1} in 2014 (Fig. 5*A*). However, in RT2 (the larger group), C_i decreased remarkably until about 1975 (at $C_a \cong 330$ µmol mol^{-1}) and started to increase in the early 1990s (at $C_a = 355$ µmol mol^{-1}). C_i in RT2 was 20–30 µmol mol^{-1} higher than in RT1 by at the extremes (one hundred years ago and today) but reached values slightly below those of RT1 at the minima (1975–1995).

The long-term course of C_i/C_a also showed two different patterns. In RT1, C_i/C_a annual averages remained almost unchanged over the last century (0.53 ± 0.03, mean ± SD; *ANOVA*: $F(2,40) = 0.72$, p=0.49) (Fig. 5*B*). In RT2, C_i/C_a values fluctuated: they were high before 1975 (0.59 ± 0.05), then declined to slightly lower values than in RT1 in the period 1975–1995 (0.51 ± 0.01), and increased again substantially in the last two decades (0.56 ± 0.02; *ANOVA*: $F(2,88) = 11.4$, $p<0.001$). Any value of s except $s \geq 1$ generates an increase in WUE_i with increasing C_a (Fig. 2*D*). The only period in which WUE_i did not change remarkably ($s = 1$ and $C_a - C_i = 0$) was after the year 2000 in RT2 (Fig. 5*C*).

Trees adjusted their C_i in response to increasing C_a and changing climate in a manner that was specific to RT and/or altitude of the growth site. In RT1, s increased from slightly negative values in the first decades of the last century to 1 in 2014 (average $s = 0.42$, Fig. 6*A*), meaning that C_i increased by 0.43 µmol mol^{-1} for every increment of 1 µmol mol^{-1} in C_a during the last hundred years. In contrast, C_i in RT2 declined by 100% of the C_a increment until 1974 (averaged over all elevations:

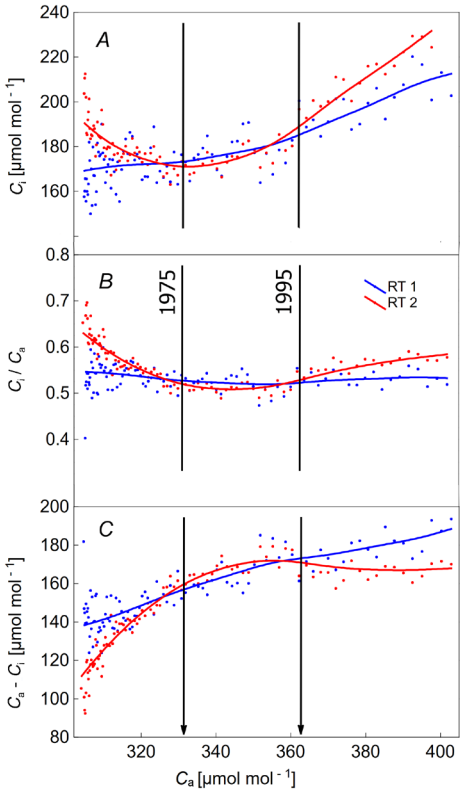

Fig. 5. Responses of C_i and related parameters (C_i/C_a ratio and $C_a - C_i$ difference) to increasing atmospheric CO_2 concentration (C_a) in Norway spruce needles. The range of CO_2 concentrations on the abscissa (~300–400 µmol mol^{-1}) covers the increase in C_a between 1911 and 2015. The C_i values were inferred from the carbon isotope ratio ($\delta^{13}C$) in the cellulose of tree rings from trees grown in Central Europe (*see* Fig. 1 for sampling sites). The C_a values were obtained from published meteorological and ice-core data. Each point represents the annual average of n = 2–22 trees from the RT1 group (*blue*) or n = 2–35 trees from the RT2 group (*red*) (the smaller n applies to older trees). *The lines* are distance-weighted least-square fits with a stiffness of 0.25. *The vertical lines* separate three periods with significantly different response shapes in the RT groups. The difference $C_a - C_i$ in panel *C* is equivalent to $WUE_i \times 1.6$.

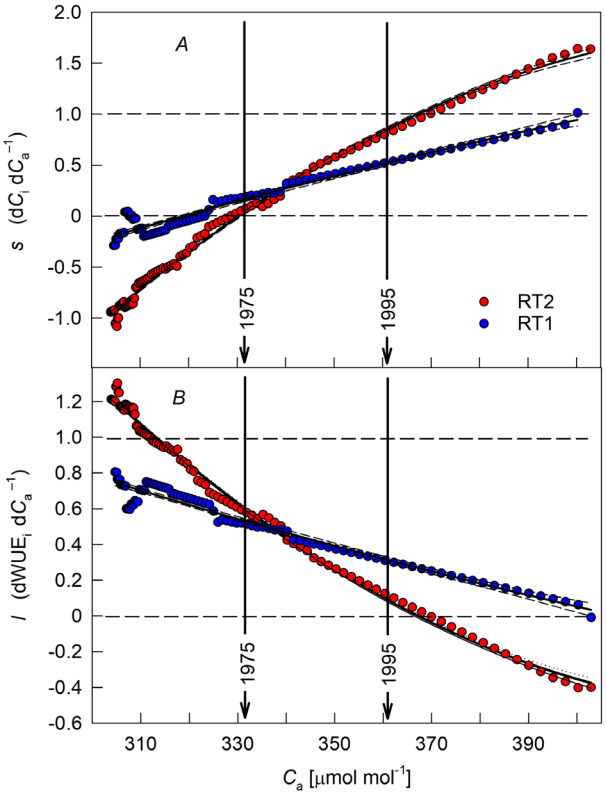

Fig. 6. Sensitivity of C_i and WUE_i to centennial increase in the atmospheric CO_2 concentration C_a. The sensitivity s of the C_i response to C_a (dC_i/dC_a) increased (*A*) and the sensitivity l of WUE_i to elevating C_a ($dWUE_i/dC_a$) decreased (*B*) during the 20th century. The s and l of the RT1 trees scaled between 0 and 1, but in the RT2 group of trees s and l exceed these limits, indicating a steep increase in WUE_i at the beginning of the century and an insensitivity or even a decrease in WUE_i during the last decades. *The coloured circles* show the means of s for each C_a (year) across all analysed tree-ring cores. The C_a-course of s was calculated for each core as the derivative of the polynomial fit through the C_i values plotted against C_a. The average r^2 across 34 and 23 fits in RT2 and RT1 was 0.70 and 0.47, respectively. *The solid* and *dotted lines* are regression lines through the means and 95% confidence intervals, respectively.

s = –1.00, *see* Table 1S, *supplement*), increased slightly in the intermediate period 1975–1994 (s = +0.40) and rose at almost the same rate as C_a in the last 20 years (1995–2014) (s = +0.87); it exceeded s = 1 in 2000 and continued to increase in the following 14 years.

Intrinsic water-use efficiency (WUE_i): As expected, WUE_i increased over the last 90–100 years. While C_a rose by 29% (from 303 µmol mol^{-1} in 1920 to 393 µmol mol^{-1} in 2010), WUE_i increased by 46% in the same period [from 74 ± 5 to 109 ± 4 µmol(CO_2) mol^{-1}(H_2O); mean ± SD]. However, C_i rose at a different rate than C_a, or even declined (s < 0), so that the drawdown of CO_2 concentration from the atmosphere to the leaf interior, $C_a - C_i$, which is proportional to WUE_i, differed as a function of RT (Fig. 5*C*). Trees classified as different RT differed significantly in WUE_i in the periods 1920–1974 and 1995–2014, but not during 1975–1994 (Fig. 7).

Interestingly, WUE_i in RT1 deviated between the high- and low-altitude sites by 19.8 µmol mol^{-1} (p=0.001), with higher values in the lower (<700 m a.s.l.) than the (sub) montane areas (>700 m a.s.l.). In RT2, WUE_i increased curvilinearly with a quasi-linear steep rise in 1920–1974, a continuously declining slope in 1975–1994 and a final slight linear decrease in 1995–2014 (Figs. 5*C*, 7). The change in WUE_i per C_a unit ($dWUE_i/dC_a$, slope l) was fairly stable in RT1 ($0.23 < l < 0.67$, mean l = 0.43), independently of elevation and C_a (Table 1S, Fig. 6*B*). In RT2, WUE_i was much more sensitive to increasing C_a in 1920–1970, when l amounted to 1.12 mol(air) mol^{-1}(H_2O).The sensitivity decreased to 0.38 mol(air) mol^{-1}(H_2O) in 1975–1994 and remained close to zero at 0.08 mol(air) mol^{-1}(H_2O) during 1995–2014 (Table 1S). Interpolated values of WUE_i in RT1 and RT2 groups for each core, altitude, and year are shown in Fig. 4S (*supplement*).

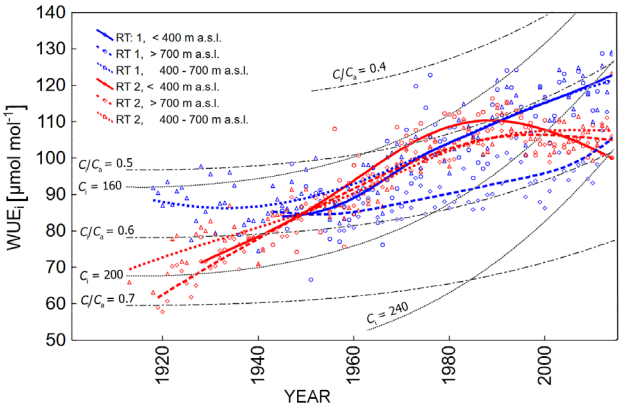

Fig. 7. Centennial trajectories of intrinsic water-use efficiency (WUE_i) of Norway spruce trees reconstructed from the stable carbon isotope ratio ($\delta^{13}C$) in the late-wood cellulose of tree-rings. The Response Types (RT) were subdivided according to the elevation of the sampling (*i.e.*, growth) sites into a mountain (>700 m a.s.l.), middle altitude (400–700 m a.s.l.) or low altitude (<400 m a.s.l.) elevations. The WUE_i at the mountain sites of RT1 (*blue diamonds* and *blue dashed line*) was lower than that at middle and low altitudes (*blue triangles*, *dotted lines* and *circles*, *solid lines*, respectively), while no such differences occurred in RT2 (*red symbols* and *lines*). *The symbols* represent annual averages; *the lines* are distance-weighted least-square fits with a stiffness of 0.25. *The black lines* show the simulated WUE_i time courses at constant C_i values (*dotted lines*) and constant C_i/C_a ratio values (*dash-dot lines*).

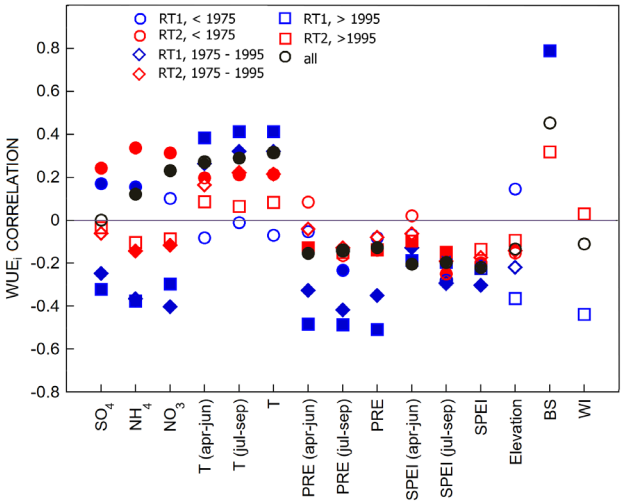

Fig. 8. Correlation coefficients of intrinsic water-use efficiency (WUE_i) of Norway spruce with selected environmental factors in three time periods between 1919 and 2014. Trees were divided into two categories, Response Types 1 and 2 (RT1, RT2), according to their temporal response of $\Delta^{13}C$ to C_a. WUE_i was inferred from $\Delta^{13}C$ in the tree rings (Eq. 3 in "Materials and methods"). The matrix shows the WUE_i correlations for the different time periods indicated with annual deposition rates (SO_4^{2-}, NH_4^+, NO_3^-), air temperature during spring [T (Apr–Jun)], summer [T (Jul–Sep)] and the whole year (T), total precipitation (PRE) and the standard precipitation and evaporation index (SPEI) with the same seasonal specification, elevation of tree growth sites (Elevation), saturation of the soil with basic cations such as Ca^{2+}, Mg^{2+}, K^+ (BS) and total wood increment per hectare and year (WI). The factors with statistically significant correlations ($p<0.05$) are marked with *closed symbols*; *open symbols* indicate $p>0.05$; positive and negative values of the correlation coefficients indicate proportional and indirect (negative) relationships with WUE_i, respectively. All data are site (tree)-specific; the BS and WI data were available only for the most recent period (1995–2014), and all other data were obtained from direct instrumental measurements or modelling for the entire study period (1919–2014).

The effect of the environment on WUE_i: We attempted to identify an environmental cause for the differences between RT1 and RT2. *Spearman*-rank correlations between WUE_i and environmental variables were calculated separately for both Response Types and three time periods (before 1975, from 1975 to 1995, and after 1995). The time series of WUE_i in RT1 showed stronger and highly significant correlations with temperature, precipitation, and the deposited amounts of sulfate (SO_4^{2-}) and nitrogen (NH_4^+ and NO_3^-) in comparison with the RT2 series (Fig. 8). The highest correlations were usually found for the most recent period (>1995). As expected, precipitation correlated negatively with WUE_i, irrespective of whether monthly or annual mean precipitation values were used. Higher air temperatures led to higher WUE_i. The deposition of pollutants correlated negatively with the WUE_i in RT1, as higher deposition rates resulted in lower WUE_i; in RT2, however, higher deposition rates increased the WUE_i by 1975.

Discussion

The time series of C_i derived from the ^{13}C content in the tree rings allowed us to reconstruct the WUE_i patterns in the C_a-changing environment. The persistent centennial increase in C_a manifested as an increase in C_i and/or an increasing $C_a - C_i$ difference proportional to WUE_i in Norway spruce. In addition to this commonly observed phenomenon, an opposite trend has also emerged – a decrease in C_i or a reduction in WUE_i with increasing C_a over certain periods. In most of our trees (the group that designed RT2), WUE_i peaked between the 1970s and the early 1990s and plateaued or declined slightly after 2000. In about one-third of the trees (RT1), WUE_i has been steadily increasing for about 100 years. The presence of two distinct response patterns of C_i and WUE_i, requiring remarkable differences in the century-long history of stomatal conductance and photosynthetic rates, raises several questions: (*1*) How does the long-term rise in C_a impact WUE_i and the strategy of spruce to control C_i? (*2*) What underlies the difference between RTs? (*3*) What are water use and spruce growth prospects in the coming decades?

How does the long-term rise in C_a impact WUE_i?: The leaf's internal CO_2 concentration results from the balanced net CO_2 assimilation rate P_N, *i.e.*, the carboxylation rate in chloroplasts reduced by the (photo)respiration rate, and the net CO_2 flux through stomata, which is proportional to the stomatal conductance g_s. It has been commonly observed that g_s is reduced and water is saved in plants

growing under elevated CO_2. Typically, a doubling of C_a in growth cabinets, open-top chambers or FACE experiments leads to a short-term reduction of g_s by 10–40%. Medlyn *et al.* (2001) and Ainsworth and Rogers (2007) arrived at similar values of 21–22% reduction in g_s averaged over C_3 and C_4 grasses, crops, shrubs, and forest trees in their meta-analyses. Trees growing at C_a of 567 µmol mol^{-1} showed a 19% decrease in mean g_s value compared to C_a of 366 µmol mol^{-1}. Young trees usually respond more strongly. In mature trees, the situation is ambiguous (Körner 2003, Leuzinger and Körner 2007). If P_N remains unchanged and g_s is reduced by 19%, as in Ainsworth and Rogers (2007), the WUE_i of the trees can be expected to increase by 23% (to 1/0.81 × 100 = 123.4%). Averaged over all our trees, WUE_i increased by 46% over the last 100 years (31.1% for RT1 and 60.2% for RT2), suggesting, to a first approximation, higher stomatal closure and/or increased P_N during the centennial increase in C_a. Based on the same metadata analyses, the light-saturated P_N increased by about 46% in trees grown at elevated C_a (567 *vs*. 366 µmol mol^{-1} in the control) (Ainsworth and Rogers 2007). Thus, the partial effect of P_N on WUE_i at invariable g_s would be 46%. With a simultaneous reduction in g_s and an increase in P_N, an 80% increase in WUE_i (to 1.46/0.81 × 100 = 180.2%) can be expected. Considering the doubling of C_a in the aforementioned meta-analysis compared to the increase in C_a between 1913 and 2014 for which we have WUE_i data, the expected 40% increase in WUE_i based on the metadata (80/2) corresponds well to the 46% increase found here.

Our data indicate that WUE_i depends on altitude. As expected, WUE_i at RT1 was significantly higher on drier and warmer low-elevations plots than on wetter and cooler stands at high elevations (Fig. 7). The likely reasons for this are a low-temperature limitation of P_N and water shortage or a high VPD limitation of g_s. It is a widespread observation that WUE_i follows a gradient of precipitation and/or VPD (Maseyk *et al.* 2011, Oulehle *et al.* 2023). In contrast, WUE_i in RT2 did not correlate significantly with altitude and associated environmental factors.

***C_i* control strategies**: Detailed analyses of C_i variation with increasing C_a are rare (Feng 1998, Seibt *et al.* 2008, McCarroll *et al.* 2009, Maseyk *et al.* 2011). We found all common scenarios of the C_i *vs*. C_a relationship in our samples. In the RT1 trees, C_i rose on average by 42% of the C_a increase and the increase was monotonic over the last 100 years (Fig. 5*A*). This type of response, *i.e*., the maintenance of a nearly constant C_i/C_a ratio (Fig. 5*B*), which is typical for plants balancing CO_2 supply on the verge of the photosynthetic limitation by Rubisco activity and RuBP regeneration, has already been described by Wong *et al.* (1985) and suggests possible signal transduction from the CO_2-assimilating mesophyll to the stomata in the epidermis. C_i/C_a homeostasis has also been found in response to long-term CO_2 elevation, suggesting that photosynthesis and stomata acclimate to elevating C_a in tandem (Drake *et al.* 1997, Feng 1998, Andreu-Hayles *et al.* 2011, Gagen *et al.* 2011). On developmental and evolutionary time scales, the stability of the C_i/C_a ratio indicates a balanced partitioning of nitrogen between Rubisco and RuBP regeneration enzymes coordinated with stomatal development (Franks *et al.* 2013). This most common C_i control strategy encompasses the entire range of C_i sensitivities s higher than 0 and lower than 1 (scenario *B* in Fig. 2). This has been the predominant mode of C_i adjustment in RT1 over the last hundred years.

In contrast, RT2 trees changed the strategy of C_i and WUE_i control during their lifetime by successively using four scenarios shown in Fig. 2: C_i remains nearly constant regardless of C_a ($s = 0$, panel *A*); C_i increases by a fraction s of the C_a increment ($0 < s < 1$, *B*); C_i mirrors the C_a increment, *i.e*., $C_a - C_i$ and WUE_i remain constant ($s = 1$, *C*); and, to a limited extent, C_i increases faster than C_a ($s > 1$, *D*). Remarkably, s was even negative in RT2 trees for two-thirds of the last century (C_i decreased with rising C_a). While four of the five modes of C_i and WUE_i control encountered here have also been found in many other studies (*see* "Introduction" for references), one appears to be unusual for the literature: a steady decline in C_i despite an increase in C_a over six decades (*see* the negative slopes s in RT2 for all elevations in Table 1S and Fig. 6*A*). This type of response, which occurs as a result of stomata closing enough to decrease C_i, is presented schematically in Fig. 7S (*supplement*), assuming that the P_N parameters, *i.e*., the maximum carboxylation rate $V_{c\,max}$ and maximum electron transport rate in the thylakoid membranes J_{max}, have not changed substantially [*see* the small tree-specific reduction of both $V_{c\,max}$ and J_{max} at elevated C_a in Ainsworth and Rogers (2007)]. Apparently, under these circumstances, saving water through a large reduction in stomatal conductance dominates tree behaviour at the expense of carbon assimilation. Water shortage and/or increased evaporation demand from the atmosphere are the likely reasons for this. However, according to Brienen *et al.* (2017), tree height associated with changes in stem and leaf hydraulics and crown irradiation can be responsible for the C_i depressions accompanying the C_a increase. The authors observed this effect in three broadleaf species, but not *Pinus*. There could therefore be a specificity with the species (angiosperms *vs*. conifers) and/or the habitat.

The lack of a single homeostatic response (constant C_i, C_i/C_a or $C_a - C_i$) and instead the dynamic "shift along a continuum of these strategies" with the $C_a - C_i$ drawdown constant at high C_a levels was also reported by Voelker *et al.* (2016) for a large set of paleo- and CO_2-enrichment studies with gymnosperms and angiosperms. What underlies the shifts in the relationship between C_i and C_a and the changes in s and WUE_i with increases in C_a? The slope s, the sensitivity with which C_i changes in response to C_a (dC_i/dC_a), represents the strength with which plants control C_i (Farquhar *et al.* 1978) and is prone to environmental impacts (Santrucek and Sage 1996). Plants with $s = 0$ "protect" the leaf so strongly that no changes in C_i occur in response to rising C_a due to stomatal closure; thus, they exhibit C_i homeostasis and $s = 0$ indicates water shortage as mentioned above. In contrast, plants with $s = 1$ allow C_i to "passively" follow C_a (and $C_a - C_i$ remains constant). Low strength ($s = 1$) likely diagnoses saturation

of photosynthesis in addition to stomata approaching the upper affordable value of their opening. We show here that *s* ranged from –0.2 to 1 for RT1 and from –1.00 to 1.6 for RT2 but increased in both groups with C_a rising over the last hundred years (Fig. 6*A*). Clearly, the strength of the mechanisms controlling C_i has gradually waned with the long-term gradual elevation of atmospheric CO_2. How does this loss of control strength relate to the development of the tree (age) and its environment?

Developmental factors that influence *s*: Age-related traits, particularly increasing size, height, and the resulting build-up of hydraulic resistance of trees, can influence stomatal conductance and impair or mask the influence of C_a or other environmental factors on C_i and WUE_i. This so-called "juvenile effect", which usually occurs in the initial several decades of a tree's life, has been frequently observed (McCarroll and Loader 2004, McCarroll *et al.* 2009). Its duration is species-specific (Gagen *et al.* 2008, Duffy *et al.* 2017) and can extend over several centuries in extremely tall and millennial coast redwood (Voelker *et al.* 2018). Recently, Brienen *et al.* (2017) attributed changes in tree-ring $\delta^{13}C$ and an inferred increase in WUE_i to developmental changes in the trees rather than rising C_a. We attempted to eliminate the juvenile trend by discarding the rings with a cambial age of less than 30 years in all trees and analysing only the cores of trees older than 63 years. We found no significant differences in tree height between the RT1 and RT2 groups. Thus, it is unlikely that the interannual variations in C_i and WUE_i observed here or the differences in the time course of *s* between the RT1 and RT2 trees are simply due to the age or size-related characteristics of the trees.

Environmental factors affecting sensitivities *s* and *l*: Global warming, increase in VPD, higher frequency of heat waves or global reduction in wind speed all affect leaf, canopy, and ecosystem gas exchange and may result in enhanced water loss and reduced carbon gain (Coumou *et al.* 2015, Schymanski and Or 2016, Menezes-Silva *et al.* 2019, Cernusak 2020, Novick *et al.* 2024). Indeed, the reduced vitality of spruce trees due to acute or chronic drought, wind, and air pollutants and the resulting susceptibility to pest infestation have been identified as causes of tree mortality and forest decay (Venäläinen *et al.* 2020). The time course of *s* and WUE_i could help to diagnose drought and carbon starvation as the cause of tree mortality (Sala *et al.* 2010). Negative values of *s* accompanied by increasing WUE_i indicate long-term water saving, stomata closure, and a deficit of newly synthesised assimilates when they occur in consecutive years. This probably happened to our RT2 trees in the first half of the last century. However, as WUE_i reached a plateau in the late 1980s and in the 1990s and *s* approached 1, the trees seem to have coped with the adverse conditions. The demand for increased water saving vanishes, C_i "passively" follows C_a and WUE_i does not change with time. Moreover, $s > 1$ indicates an "overreaction", when C_i increases faster than C_a: the capacity of the photosynthetic apparatus to fix CO_2 does not keep pace with the increasing capacity of CO_2 transport pathways and elevating C_a. Consequently, stomatal conductance (and likely transpiration rate) increases without a corresponding increment in photosynthetic rate and, thus, WUE_i remains constant or even decreases. The sensitivity *l* of WUE_i to a change in C_a, $dWUE_i/dC_a$, is zero or negative as shown in Fig. 6*B*. This trend of decreasing *l* over the last century has also recently been observed on a global scale. Adams *et al.* (2020) extracted ^{13}C data from 422 tree-ring series of angiosperm and gymnosperm species from around the world and reported a significant decrease in *l* over the last century: in 1965, before the rapid rise in C_a, *l* averaged 0.34, whereas it dropped to 0.25 with the onset of the rapid exponential increase in C_a between 1965 and 2000. Here, *l* decreased from 0.70 to 0.46 for RT1 and from 1.09 to 0.46 for RT2 during the same periods, and the depression continued after 2000, especially for RT2 trees with negative *l* values (Fig. 6*B*). The reduction of *l* under global C_a elevation has recently been discussed (Adams *et al.* 2020), but the underlying mechanisms are not fully understood. Likely, the CO_2-closing effect on stomata is less pronounced, and long-term CO_2 fertilisation becomes ineffective or even inhibitory in photosynthetic carbon fixation.

Nutrient limitation, particularly the availability of nitrogen, has often been shown to constrain the maximum photosynthetic rates in a CO_2-enriched atmosphere (Ainsworth and Long 2005) and underlies the correlation of N deposition with WUE_i (Saurer *et al.* 2014). Although Rubisco operates in a non-CO_2-saturated environment, photosynthetic rate and tree growth can be limited by nitrogen or phosphorus deficiency (Körner 2006, Rennenberg *et al.* 2009). In conifers, Rubisco can serve as a nitrogen storage especially in autumn when Rubisco is synthesized over carbon fixation and a Rubisco pool with limited activity can form (Millard and Grelet 2010). From this perspective, nitrogen is likely remobilized and invested in the reorganized photosynthetic apparatus in a variable pattern each spring, depending on nitrogen deposition, carbon supply, water and other sources availability. Even nutrients such as calcium (Ca), without any dominant role in the photosynthetic carbon fixation machinery, can affect WUE_i if poorly available in soils affected by acid rain (Oulehle *et al.* 2023). This mechanism could contribute to the remarkably high positive correlation of WUE_i with soil saturation with basic cations in RT1 (Fig. 8). Surprisingly, it has also been suggested that a global depression of wind speed (Coumou *et al.* 2015) reduces WUE (the ratio of net photosynthetic rate P_N to transpiration rate *E*) and counteracts the rise in WUE with increasing CO_2 (Schymanski and Or 2016).

What may underlie the differences between the Response Types?: We found two notable differences that distinguish the trees in the RT1 and RT2 categories. First, the time courses and C_a dependencies of their C_i and C_i-derived values differed (Fig. 5). Second, ^{13}C and related traits show RT-specific interannual variability among trees: RT2 trees showed smaller standard deviations (SD) of $\Delta^{13}C$ than RT1 trees over the past century, although the difference diminished as C_a approached present-day

values (Fig. 8S, *supplement*). The lack of responsiveness of RT2 is also indicated by the weak correlations between WUE_i and various environmental cues and the remarkably lower SD of tree-ring width in RT2 than in RT1 (Fig. 5S*B*). On the other hand, tree height and age did not differ between RT groups (data not shown).

We have not found a single environmental parameter that explains the differences between the Response Types. RT1 and RT2 cannot be separated by the altitude of growth sites, soil texture or chemistry. Interestingly, the RT1 group showed statistically significant correlations with many environmental variables, including recent and site-specific variations in soil chemistry (base saturation) and wood increment. The reason for the lack of responsiveness of RT2 is not clear. We suggest a possible long-term limitation of carbon gain and subsequent carbon starvation due to shortage of water or excessive water loss and chronic stomata closure. An individual, perhaps genetically determined, high response threshold to an environmental stressor, such as water shortage, nitrogen deficiency or excessive pollutants, could predispose individual trees to such limitation. However, our results indicate that site-specific environmental conditions outweigh the genome specificity of individual trees. It is difficult to predict the gas exchange and growth strategy of trees in the future when atmospheric CO_2 concentration continues to increase and pollutant deposition decreases. Extrapolation of the time course of the sensitivities of C_i and WUE_i (s and l) predicts a continuous decrease of WUE_i rise, insensitivity or even a WUE_i decrease in the next decades.

To summarize, spruce trees responded to the century-long increase in atmospheric CO_2 in two distinctly different patterns. In the first group, RT1, trees continuously increased their WUE_i, and their value was higher in low-altitude habitats (higher temperature and lower precipitation) than in cooler and wetter mountain regions. The leaf's internal CO_2 concentration increased with the atmospheric concentration, so the C_i/C_a ratio remained fairly constant. Each C_a increment resulted in an increase in C_i by 43% of the C_a increment ($s = dC_i/dC_a = 0.43$) in the century average. However, the sensitivity of s increased over time, reaching almost 1 after 2000, indicating that the increase in WUE_i ceased over time, probably due to invariant photosynthesis and stomatal conductance. In the second group of trees, RT2, C_i decreased during the first seven decades of tree ontogeny, although C_a increased concomitantly, leading to a strong rise in WUE_i. This could be caused by a decrease in g_s due to water shortage or a rise in hydraulic resistance accounted to the rapid growth of the trees. Alternatively, the increased rate of photosynthesis due to direct sunlight on the crown could also play a role. Interestingly, the sharp decline in growth of WUE_i that coincided with the peak of pollution – sulfur and nitrogen deposition – in the 1980s and 1990s was followed by a saturation of WUE_i and even a slight decline after 2000. In all our spruce trees, environmental conditions, likely light and VPD microenvironment, air pollution and soil properties, outweighed genetic differences between trees in determining WUE_i. The sensitivity of WUE_i to increasing C_a ($l = dWUE_i/dC_a$) decreased during tree ontogeny, suggesting that an equilibrium between carbon gain and water loss was established at the whole-tree level.

References

Adams M.A., Buckley T.N., Turnbull T.L.: Diminishing CO_2-driven gains in water-use efficiency of global forests. – Nat. Clim. Change **10**: 466-471, 2020.

Ainsworth E.A., Long S.P.: What have we learned from 15 years of free-air CO_2 enrichment (FACE)? A meta-analytic review of the responses of photosynthesis, canopy properties and plant production to rising CO_2. – New Phytol. **165**: 351-371, 2005.

Ainsworth E.A., Rogers A.: The response of photosynthesis and stomatal conductance to rising [CO_2]: mechanisms and environmental interactions. – Plant Cell Environ. **30**: 258-270, 2007.

Altman J., Fibich P., Santruckova H. *et al.*: Environmental factors exert strong control over the climate-growth relationships of *Picea abies* in Central Europe. – Sci. Total Environ. **609**: 506-516, 2017.

Andreu-Hayles L., Planells O., Gutiérrez E. *et al.*: Long tree-ring chronologies reveal 20th century increases in water-use efficiency but no enhancement of tree growth at five Iberian pine forests. – Glob. Change Biol. **17**: 2095-2112, 2011.

Arco Molina J.G., Saurer M., Altmanova N. *et al.*: Recent warming and increasing CO_2 stimulate growth of dominant trees under no water limitation in South Korea. – Tree Physiol. **44**: tpae 103, 2024.

Baillie M.G.L., Pilcher J.R.: A simple crossdating program for tree-ring research. – Tree-Ring Bull. **33**: 7-14, 1973.

Betts R.A., Boucher O., Collins M. *et al.*: Projected increase in continental runoff due to plant responses to increasing carbon dioxide. – Nature **448**: 1037-1041, 2007.

Boettger T., Haupt M., Friedrich M., Waterhouse J.S.: Reduced climate sensitivity of carbon, oxygen and hydrogen stable isotope ratios in tree-ring cellulose of silver fir (*Abies alba* Mill.) influenced by background SO_2 in Franconia (Germany, Central Europe). – Environ. Pollut. **185**: 281-294, 2014.

Brienen R.J.W., Gloor E., Clerici S. *et al.*: Tree height strongly affects estimates of water-use efficiency responses to climate and CO_2 using isotopes. – Nat. Commun. **8**: 288, 2017.

Brümmer C., Black T.A., Jassal R.S. *et al.*: How climate and vegetation type influence evapotranspiration and water use efficiency in Canadian forest, peatland and grassland ecosystems. – Agr. Forest Meteorol. **153**: 14-30, 2012.

Buras A., van der Maaten-Theunissen M., van der Maaten E. *et al.*: Tuning the voices of a choir: detecting ecological gradients in time-series populations. – PLoS ONE **11**: e0158346, 2016.

Čada V., Šantrůčková H., Šantrůček J. *et al.*: Complex physiological response of norway spruce to atmospheric pollution – decreased carbon isotope discrimination and unchanged tree biomass increment. – Front. Plant Sci. **7**: 805, 2016.

Cavender-Bares J., Bazzaz F.A.: Changes in drought response strategies with ontogeny in *Quercus rubra*: implications for scaling from seedlings to mature trees. – Oecologia **124**: 8-18, 2000.

Cernusak L.A.: Gas exchange and water-use efficiency in plant canopies. – Plant Biol. **22**: 52-67, 2020.

Cienciala E., Russ R., Šantrůčková H. *et al.*: Discerning environmental factors affecting current tree growth in Central

Europe. – Sci. Total Environ. **573**: 541-554, 2016.
Coumou D., Lehmann J., Beckmann J.: The weakening summer circulation in the Northern Hemisphere mid-latitudes. – Science **348**: 324-327, 2015.
Cowan I.R., Farquhar G.D.: Stomatal function in relation to leaf metabolism and environment. – In: Jennings D.H. (ed.): Integration of Activity in the Higher Plant. Pp. 471-505. The University Press, Cambridge 1977.
Drake B.G., Gonzalez-Meler M.A., Long S.P.: More efficient plants: A consequence of rising atmospheric CO_2? – Annu. Rev. Plant Phys. **48**: 609-639, 1997.
Duffy J.E., McCarroll D., Barnes A. *et al.*: Short-lived juvenile effects observed in stable carbon and oxygen isotopes of UK oak trees and historic building timbers. – Chem. Geol. **472**: 1-7, 2017.
Eckstein D., Bauch J.: Beitrag zur Rationalisierung eines dendrochronologischen Verfahrens und zur Analyse seiner Aussagesicherheit. – Forstwiss. Centralbl. **88**: 230-250, 1969.
Farquhar G.D., Dubbe D.R., Raschke K.: Gain of feedback loop involving carbon dioxide and stomata: theory and measurement. – Plant Physiol. **62**: 406-412, 1978.
Farquhar G.D., Ehleringer J.R., Hubick K.T.: Carbon isotope discrimination and photosynthesis. – Annu. Rev. Plant Phys. **40**: 503-537, 1989.
Farquhar G.D., O'Leary M.H., Berry J.A.: On the relationship between carbon isotope discrimination and the intercellular carbon dioxide concentration in leaves. – Aust. J. Plant Physiol. **9**: 121-137, 1982.
Farquhar G.D., Sharkey T.D.: Stomatal conductance and photosynthesis. – Annu. Rev. Plant Biol. **33**: 317-345, 1982.
Feng X.H.: Long-term c_i/c_a response of trees in western North America to atmospheric CO_2 concentration derived from carbon isotope chronologies. – Oecologia **117**: 19-25, 1998.
Francey R.J., Allison C.E., Etheridge D.M. *et al.*: A 1000-year high precision record of $\delta^{13}C$ in atmospheric CO_2. – Tellus B **51**: 170-193, 1999.
Francey R.J., Farquhar G.D.: An explanation of $^{13}C/^{12}C$ variations in tree rings. – Nature **297**: 28-31, 1982.
Frank D.C., Poulter B., Saurer M. *et al.*: Water-use efficiency and transpiration across European forests during the Anthropocene. – Nat. Clim. Change **5**: 579-583, 2015.
Franks P.J., Adams M.A., Amthor J.S. *et al.*: Sensitivity of plants to changing atmospheric CO_2 concentration: from the geological past to the next century. – New Phytol. **197**: 1077-1094, 2013.
Fritts H.C.: Tree Rings and Climate. Pp. 567. Academic Press, New York 1976.
Gagen M., Finsinger W., Wagner-Cremer F. *et al.*: Evidence of changing intrinsic water-use efficiency under rising atmospheric CO_2 concentrations in Boreal Fennoscandia from subfossil leaves and tree ring delta ^{13}C ratios. – Glob. Change Biol. **17**: 1064-1072, 2011.
Gagen M., McCarroll D., Robertson I. *et al.*: Do tree ring $\delta^{13}C$ series from *Pinus sylvestris* in northern Fennoscandia contain long-term non-climatic trends? – Chem. Geol. **252**: 42-51, 2008.
Gärtner H., Nievergelt D.: The core-microtome: A new tool for surface preparation on cores and time series analysis of varying cell parameters. – Dendrochronologia **28**: 85-92, 2010.
Gebauer G., Schulze E.-D.: Carbon and nitrogen isotope ratios in different compartments of a healthy and a declining *Picea abies* forest in the Fichtelgebirge, NE Bavaria. – Oecologia **87**: 198-207, 1991.
Gessler A., Ferrio J.P., Hommel R. *et al.*: Stable isotopes in tree rings: towards a mechanistic understanding of isotope fractionation and mixing processes from the leaves to the wood. – Tree Physiol. **34**: 796-818, 2014.
Guerrieri R., Mencuccini M., Sheppard L.J. *et al.*: The legacy of enhanced N and S deposition as revealed by the combined analysis of $\delta^{13}C$, $\delta^{18}O$ and $\delta^{15}N$ in tree rings. – Glob. Change Biol. **17**: 1946-1962, 2011.
Hetherington A.M., Woodward F.I.: The role of stomata in sensing and driving environmental change. – Nature **424**: 901-908, 2003.
Hoshika Y., Omasa K., Paoletti E.: Whole-tree water use efficiency is decreased by ambient ozone and not affected by O_3-induced stomatal sluggishness. – PLoS ONE **7**: e39270, 2012.
Jasechko S., Sharp Z.D., Gibson J.J. *et al.*: Terrestrial water fluxes dominated by transpiration. – Nature **496**: 347-350, 2013.
Keeling C.D., Whorf T.P.: Atmospheric CO_2 Records from Sites in the Scripps Institution of Oceanography (SIO) Air Sampling Network (1985–2007). CDIAC, ESS-DIVE repository 2004. *Available at*: https://data.ess-dive.lbl.gov/datasets/doi:10.3334/CDIAC/ATG.NDP001.
Keenan T.F., Hollinger D.Y., Bohrer G. *et al.*: Increase in forest water-use efficiency as atmospheric carbon dioxide concentrations rise. – Nature **499**: 324-327, 2013.
Keller K.M., Lienert S., Bozbiyik A. *et al.*: 20th century changes in carbon isotopes and water-use efficiency: tree-ring-based evaluation of the CLM4.5 and LPX-Bern models. – Biogeosciences **14**: 2641-2673, 2017.
Köhler I.H., Macdonald A.J., Schnyder H.: Last-century increases in intrinsic water-use efficiency of grassland communities have occurred over a wide range of vegetation composition, nutrient inputs, and soil pH. – Plant Physiol. **170**: 881-890, 2016.
Körner C.: Ecological impacts of atmospheric CO_2 enrichment on terrestrial ecosystems. – Philos. T. Roy. Soc. A **361**: 2023-2041, 2003.
Körner C.: Plant CO_2 responses: an issue of definition, time and resource supply. – New Phytol. **172**: 393-411, 2006.
Lake J.A., Quick W.P., Beerling D.J., Woodward F.I.: Signals from mature to new leaves. – Nature **411**: 154, 2001.
Lake J.A., Woodward F.I.: Response of stomatal numbers to CO_2 and humidity: control by transpiration rate and abscisic acid. – New Phytol. **179**: 397-404, 2008.
Laumer W., Andreu L., Helle G. *et al.*: A novel approach for the homogenization of cellulose to use micro-amounts for stable isotope analyses. – Rapid Commun. Mass Sp. **23**: 1934-1940, 2009.
Leuzinger S., Körner C.: Water savings in mature deciduous forest trees under elevated CO_2. – Glob. Change Biol. **13**: 2498-2508, 2007.
Loader N.J., McCarroll D., Gagen M. *et al.*: Extracting climatic information from stable isotopes in tree rings. – In: Dawson T.E., Siegwolf R.T.W. (ed.): Stable Isotopes as Indicators of Ecological Change. Pp. 27-48. Elsevier, Amsterdam-Boston-Tokyo 2007.
Loader N.J., Robertson I., Barker A.C. *et al.*: An improved technique for the batch processing of small wholewood samples to α-cellulose. – Chem. Geol. **136**: 313-317, 1997.
Maseyk K., Hemming D., Angert A. *et al.*: Increase in water-use efficiency and underlying processes in pine forests across a precipitation gradient in the dry Mediterranean region over the past 30 years. – Oecologia **167**: 573-585, 2011.
McCarroll D., Gagen M.H., Loader N.J. *et al.*: Correction of tree ring stable carbon isotope chronologies for changes in the carbon dioxide content of the atmosphere. – Geochim. Cosmochim. Ac. **73**: 1539-1547, 2009.
McCarroll D., Loader N.J.: Stable isotopes in tree rings. –

Quaternary Sci. Rev. **23**: 771-801, 2004.
Medlyn B.E., Barton C.V.M., Broadmeadow M.S.J. *et al.*: Stomatal conductance of forest species after long-term exposure to elevated CO_2 concentration: a synthesis. – New Phytol. **149**: 247-264, 2001.
Menezes-Silva P.E., Loram-Lourenço L., Alves R.D.F.B. *et al.*: Different ways to die in a changing world: Consequences of climate change for tree species performance and survival through an ecophysiological perspective. – Ecol. Evol. **9**: 11979-11999, 2019.
Millard P., Grelet G.A.: Nitrogen storage and remobilization by trees: ecophysiological relevance in a changing world. – Tree Physiol. **30**: 1083-1095, 2010.
Miller-Rushing A.J., Primack R.B., Templer P.H. *et al.*: Long-term relationships among atmospheric CO_2, stomata, and intrinsic water use efficiency in individual trees. – Am. J. Bot. **96**: 1779-1786, 2009.
Novick K.A., Ficklin D.L., Grossiord C. *et al.*: The impacts of rising vapour pressure deficit in natural and managed ecosystems. – Plant Cell Environ. **47**: 3561-3589, 2024.
Oulehle F., Urban O., Tahovská K. *et al.*: Calcium availability affects the intrinsic water-use efficiency of temperate forest trees. – Commun. Earth Environ. **4**: 199, 2023.
Peñuelas J., Canadell J.G., Ogaya R.: Increased water-use efficiency during the 20th century did not translate into enhanced tree growth. – Global Ecol. Biogeogr. **20**: 597-608, 2011.
Ponton S., Flanagan L.B., Alstad K.P. *et al.*: Comparison of ecosystem water-use efficiency among Douglas-fir forest, aspen forest and grassland using eddy covariance and carbon isotope techniques. – Glob. Change Biol. **12**: 294-310, 2006.
Rennenberg H., Dannenmann M., Gessler A. *et al.*: Nitrogen balance in forest soils: nutritional limitation of plants under climate change stresses. – Plant Biol. **11**: 4-23, 2009.
Sage R.F.: Acclimation of photosynthesis to increasing atmospheric CO_2: The gas-exchange perspective. – Photosynth. Res. **39**: 351-368, 1994.
Sala A., Piper F., Hoch G.: Physiological mechanisms of drought-induced tree mortality are far from being resolved. – New Phytol. **186**: 274-281, 2010.
Santrucek J., Sage R.F.: Acclimation of stomatal conductance to a CO_2-enriched atmosphere and elevated temperature in *Chenopodium album*. – Aust. J. Plant Physiol. **23**: 467-478, 1996.
Šantrůčková H., Cienciala E., Kaňa J., Kopáček J.: The chemical composition of forest soils and their degree of acidity in Central Europe. – Sci. Total Environ. **687**: 96-103, 2019.
Šantrůčková H., Šantrůček J., Šetlík J. *et al.*: Carbon isotopes in tree rings of Norway spruce exposed to atmospheric pollution. – Environ. Sci. Technol. **41**: 5778-5782, 2007.
Saurer M., Siegwolf R.T.W., Schweingruber F.H.: Carbon isotope discrimination indicates improving water-use efficiency of trees in northern Eurasia over the last 100 years. – Glob. Change Biol. **10**: 2109-2120, 2004.
Saurer M., Spahni R., Frank D.C. *et al.*: Spatial variability and temporal trends in water-use efficiency of European forests. – Glob. Change Biol. **20**: 3700-3712, 2014.
Schweingruber F.H.: Tree Rings and Environment: Dendroecology. Pp. 609. Paul Haupt, Bern 1996.
Schymanski S.J., Or D.: Wind increases leaf water use efficiency. – Plant Cell Environ. **39**: 1448-1459, 2016.
Seibt U., Rajabi A., Griffiths H., Berry J.A.: Carbon isotopes and water use efficiency: sense and sensitivity. – Oecologia **155**: 441-454, 2008.
Tumajer J., Altman J., Štěpánek P. *et al.*: Increasing moisture limitation of Norway spruce in Central Europe revealed by forward modelling of tree growth in tree-ring network. – Agr. Forest Meteorol. **247**: 56-64, 2017.
Venäläinen A., Lehtonen I., Laapas M. *et al.*: Climate change induces multiple risks to boreal forests and forestry in Finland: A literature review. – Glob. Change Biol. **26**: 4178-4196, 2020.
Vicente-Serrano S.M., Beguería S., López-Moreno J.I.: A multiscalar drought index sensitive to global warming: the standardized precipitation evapotranspiration index. – J. Climate **23**: 1696-1718, 2010.
Vico G., Manzoni S., Palmroth S. *et al.*: A perspective on optimal leaf stomatal conductance under CO_2 and light co-limitations. – Agr. Forest Meteorol. **182-183**: 191-199, 2013.
Voelker S.L., Brooks J.R., Meinzer F.C. *et al.*: A dynamic leaf gas-exchange strategy is conserved in woody plants under changing ambient CO_2: evidence from carbon isotope discrimination in paleo and CO_2 enrichment studies. – Glob. Change Biol. **22**: 889-902, 2016.
Voelker S.L., Roden J.S., Dawson T.E.: Millennial-scale tree-ring isotope chronologies from coast redwoods provide insights on controls over California hydroclimate variability. – Oecologia **187**: 897-909, 2018.
Waterhouse J.S., Switsur V.R., Barker A.C. *et al.*: Northern European trees show a progressively diminishing response to increasing atmospheric carbon dioxide concentrations. – Quaternary Sci. Rev. **23**: 803-810, 2004.
Wong S.-C., Cowan I.R., Farquhar G.D.: Leaf conductance in relation to rate of CO_2 assimilation. I. Influence of nitrogen nutrition, phosphorus nutrition, photon flux density, and ambient partial pressure of CO_2 during ontogeny. – Plant Physiol. **78**: 821-825, 1985.
Yamaguchi D.K.: A simple method for cross-dating increment cores from living trees. – Can. J. Forest Res. **21**: 414-416, 1991.
Yu G., Song X., Wang Q. *et al.*: Water-use efficiency of forest ecosystems in eastern China and its relations to climatic variables. – New Phytol. **177**: 927-937, 2008.